

1 Electronic Supplementary Information (ESI) for

2

3 **Multifunctional polyacrylonitrile-SiO<sub>2</sub>/TiO<sub>2</sub> hollow particle**  
4 **nanofibrous membranes with robust ultra-violet-resistance and**  
5 **antibacterial effect**

6

7 *Xiayi Pan,<sup>ab</sup> Yuwei Zhu,<sup>\*b</sup> Liangdong Liu,<sup>c</sup> Changdao Mu<sup>a</sup> and To Ngai<sup>\*b</sup>*

8

9 *<sup>a</sup> Department of Pharmaceutics and Bioengineering, School of Chemical Engineering, Sichuan*

10 *University, Chengdu 610065, P. R. China*

11 *<sup>b</sup> Department of Chemistry, The Chinese University of Hong Kong, Shatin N. T., Hong Kong,*

12 *999077, P. R. China*

13 *c. O-Spheres Limited, Shatin N. T., Hong Kong, 999077, P. R. China.*

14

15 **\*Correspondence authors.**

16 **E-mail address:** [uvyzhu@gmail.com](mailto:uvyzhu@gmail.com), [tongai@cuhk.edu.hk](mailto:tongai@cuhk.edu.hk)

17

## 18 **1. Experimental section**

### 19 **1.1. Materials**

20 Polyacrylonitrile (PAN, average  $M_w=150,000$ ) was purchased from Shanghai Macklin  
21 Biochemical Co., Ltd. N, N-Dimethylformamide (DMF) was purchased from RCI Labscan Limited.  
22 Triethoxyoctylsilane (97%) was purchased from Aladdin Scientific Co., Ltd. Toluene (GR grade) was  
23 purchased from Duksan Co., Ltd.  $TiO_2$  nanoparticle (CR 828, 95% of  $TiO_2$  content) were bought from  
24 Tronox.  $SiO_2/TiO_2$  hollow particles (25% of  $TiO_2$  content) were generously provided by O-spheres  
25 Limited. All chemicals were directly used without any treatment.

26 *Escherichia coli* (*E. coli*, ATCC 8739) and *Staphylococcus aureus* (*S. aureus*, ATCC 6538) were  
27 purchased from the China Center of Industrial Culture Collection.

### 28 **1.2. Methods**

#### 29 **1.2.1. Synthesis and modification of $SiO_2/TiO_2$ hollow particles**

30 The  $SiO_2/TiO_2$  hollow particles (HPs), templated from Pickering emulsion, were generously  
31 provided by O-spheres Limited. Here, triethoxyoctylsilane was employed as surface modifier to  
32 enhance the hydrophobicity of  $SiO_2/TiO_2$  HPs. The prepared hollow particles were dispersed in  
33 toluene at a concentration of 10 mg/mL, and same concentration of triethoxyoctylsilane was added  
34 into the dispersion solution. Subsequently, the mixture was stirred at 50 °C to carry out the reaction  
35 for 4 h. Finally, the particles were centrifuged and washed by ethanol for three times and dried at  
36 60 °C to obtain the modified hollow particles (M-HPs).

#### 37 **1.2.2. Characterization of $SiO_2/TiO_2$ hollow particles and M-HPs**

38 The micromorphology of  $SiO_2/TiO_2$  hollow particles and M-HPs were observed by a scanning  
39 electronic microscopy (SEM, Phenom Pro, Thermo Scientific, USA) at the accelerated voltage of 10  
40 kV. And the average diameters of  $SiO_2/TiO_2$  hollow particles and M-HPs were measured using image

41 J software (version 1.54i) based on the SEM images. Further, TEM (Tecnai G2 Spirit Bio, FEI, USA)  
42 analysis followed by energy X-ray dispersive spectroscopy (EDS) was conducted at 120 kV, to  
43 examine the internal structure and the elemental composition of SiO<sub>2</sub>/TiO<sub>2</sub> hollow particles. The  
44 fluorescence areas of Si and Ti in the EDS mapping image were captured using ImageJ software  
45 (version 1.54i) and the content of TiO<sub>2</sub> was calculated. The chemical structures of SiO<sub>2</sub>/TiO<sub>2</sub> hollow  
46 particles and M-HPs were determined by a Fourier transform infrared spectroscopy (FT-IR, Nicolet  
47 iS10, Thermo Scientific, USA). Active radicals formed following photo-excitation of M-HPs were  
48 identified by a EPR instrument (EMX Plus, Bruker) with spin trapping agent (5,5-dimethylpyrroline-  
49 oxide (DMPO)).

### 50 **1.2.3. Fabrication of PAN/M-HPs nanofibrous membranes (PAN/M-HPs NFMs)**

51 Firstly, PAN powder was dissolved into DMF to gain homogeneous 15 wt% PAN solution with  
52 shaking for 24 h at room temperature. Secondly, the M-HPs were blended with PAN solution in  
53 different concentration (0, 1, 5 wt% (relative to PAN)) and the mixtures were sonicated until uniform  
54 suspensions were obtain. Then, the PAN/M-HPs suspension was loaded in a 10 mL syringe with a  
55 21-gauge needle and connected to the electrospinning machine (Tongli Tech Co., Limited, China).  
56 And the electrospinning process was carried out at a flow rate of 0.5 mL/h for 4 h, with a high voltage  
57 of 19 kV applied to needle, a rotate speed of receiver of 300 rpm and a working distance of 15 cm.  
58 Finally, all the prepared nanofibrous membranes were dried overnight at room temperature to allow  
59 the solvent to evaporate completely. The fabricated membranes were respectively designated as M-  
60 HPs-0, M-HPs-1 and M-HPs-5 according to the doping concentration of M-HPs.

61 Moreover, a nanofibrous membrane containing 1.25 wt% TiO<sub>2</sub> nanoparticles was set as the control  
62 group and named as TiO<sub>2</sub>-1.25, which has the same TiO<sub>2</sub> content as M-HPs-5.

### 63 **1.2.4. Characterization of PAN/M-HPs NFMs**

64 The surface morphology of the nanofibrous membranes and nanoparticles were observed by a  
65 scanning electronic microscopy (SEM, Phenom Pro, Thermo Scientific, USA). The distribution of  
66 nanoparticles in the nanofibrous membranes were further observes by using a transmission electron  
67 microscopy (TEM, Tecnai G2 Spirit Bio, FEI, USA). The average diameters of the nanofiber and  
68 nanoparticles were measured using image J software (version 1.54i) based on the SEM images. The  
69 porosity of the nanofibrous membranes were calculated by following equation<sup>1</sup>:

$$\text{Porosity (\%)} = \frac{\rho_0 - \frac{m_1}{V_1}}{\rho_0} \times 100$$

71 Where  $\rho_0$  is the density of PAN, which is 1.14 g/cm<sup>3</sup>.  $m_1$  and  $V_1$  are the weight and volume of the  
72 nanofibrous membranes, respectively.

### 73 **1.2.5. Measurements of PAN/M-HPs NFMs**

74 Ultraviolet protection factor (UPF) and UV-Vis transmittance spectra were used to evaluate the  
75 UV-resistant property of the nanofibrous membranes and nanoparticles. The UPF value were  
76 measured using a sunscreen protection factor analyzer (SPF-290AS, Solarlight, USA) according to  
77 AATCC 183-2014. And the UV-Vis transmittance spectra of the membranes and nanoparticles were  
78 obtained by a UV-Vis spectrophotometer (UV-3600 Plus, Shimadzu, Japan). In addition, rhodamine  
79 B was chosen for fluorescence attenuation experiment to evaluate the UV-resistant property of the  
80 membranes.

81 Mechanical properties were measured using a tensile machine (TOHNICHI, Zhuoyue, Dongguan,  
82 China) at a stretch rate of 20 mm/min and the tested membranes were cut into 50 mm×20 mm strips  
83 ( $n = 3$ ). Water contact angle (WCA) was measured by using a contour analysis system (OCA 25,  
84 Dataphysics, Germany) to evaluate the surface wettability of the nanofibrous membranes. The  
85 breathability was assessed using water vapor transmission rate (WVTR) according to standard ASTM

86 E96 and the test was conducted at 38 °C and 90% relative humidity.

87 *E. coli* (Gram-positive) and *S. aureus* (Gram-negative) were chosen as the model strains to  
88 investigate the antibacterial activities of the nanofibrous membranes. 20 mg of nanofibrous  
89 membranes were immersed into 5000 µL bacteria suspension ( $1 \times 10^6$  CFU) and incubated for 24 h at  
90 37 °C. Subsequently, the bacteria suspensions were diluted and their absorbance at 600 nm were  
91 measured by a UV-Vis spectrophotometer. The bacteria inhibition was calculated as following  
92 equation:

$$\text{Bacteria inhibition (\%)} = \left( \frac{\text{OD}_c - \text{OD}_t}{\text{OD}_c} \right) \times 100$$

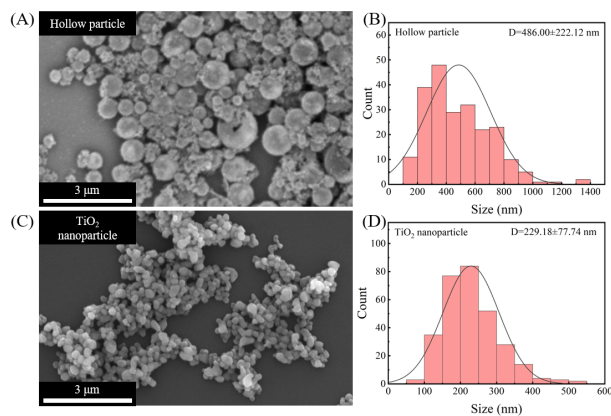
94 Where,  $\text{OD}_c$  and  $\text{OD}_t$  are the absorbance at 600 nm of the control (only bacteria suspension) and test  
95 groups, respectively.

96 In addition, the micromorphology of *E. coli* and *S. aureus* before and after contacting the  
97 nanofibrous membranes were observed by SEM (Apreo 2, Thermo Scientific, USA) at the accelerated  
98 voltage of 10 kV.

#### 99 **1.2.6. Statistical analysis**

100 All of the quantitative data were analyzed using SPSS 17.0 software for One-way analysis of  
101 variance (ANOVA) and presented as the mean  $\pm$  standard deviation. Duncan's multiple range tests  
102 was used to determine the significant differences between groups and the level of significance was  $p$   
103 value  $< 0.05$ .

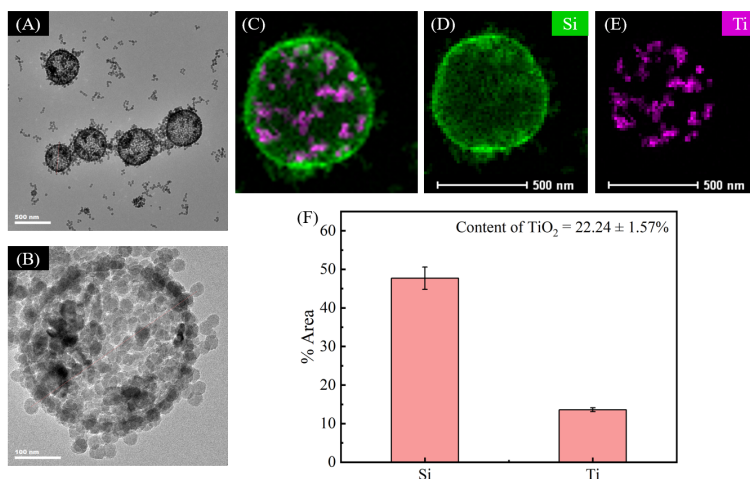
## 104 **2. Results**



105

106 **Fig. S1.** (A) SEM image and (B) particles size distribution of SiO<sub>2</sub>/TiO<sub>2</sub> hollow particles. (C) SEM  
 107 image and (D) particles size distribution of TiO<sub>2</sub> nanoparticles.

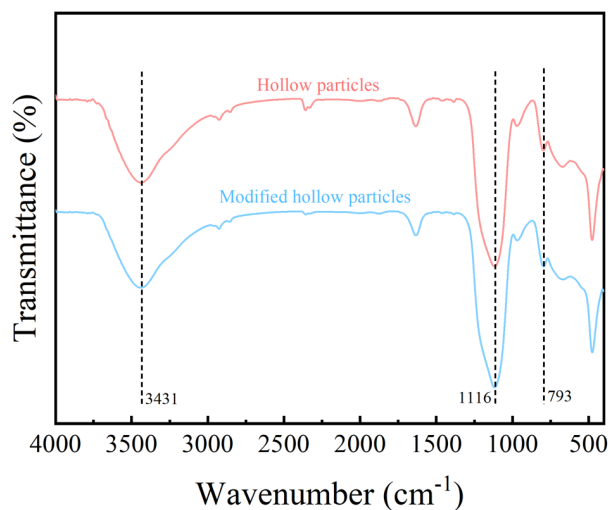
108



109

110 **Fig. S2.** (A-B) TEM images, (C-E) EDS mapping images of SiO<sub>2</sub>/TiO<sub>2</sub> hollow particles and (F)  
 111 quantitative analysis of fluorescence areas of Si and Ti.

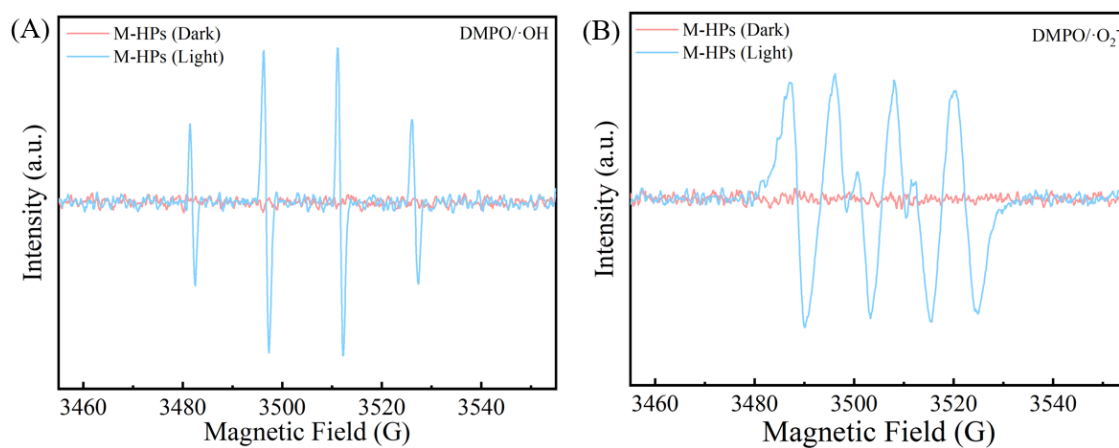
112



113

114 **Fig. S3.** FT-IR spectra of SiO<sub>2</sub>/TiO<sub>2</sub> hollow particles and modified hollow particles.

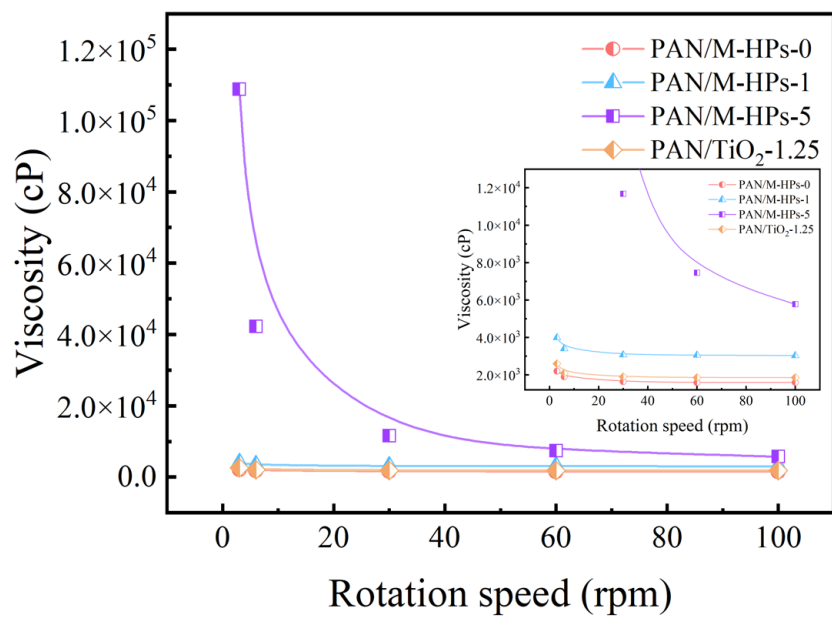
115



116

117 **Fig. S4.** EPR spectra of modified hollow particles obtained before and after light-excitation in the  
 118 presence of spin trapping agent DMPO. (A) DMPO/·OH, (B) DMPO/·O<sub>2</sub><sup>-</sup>.

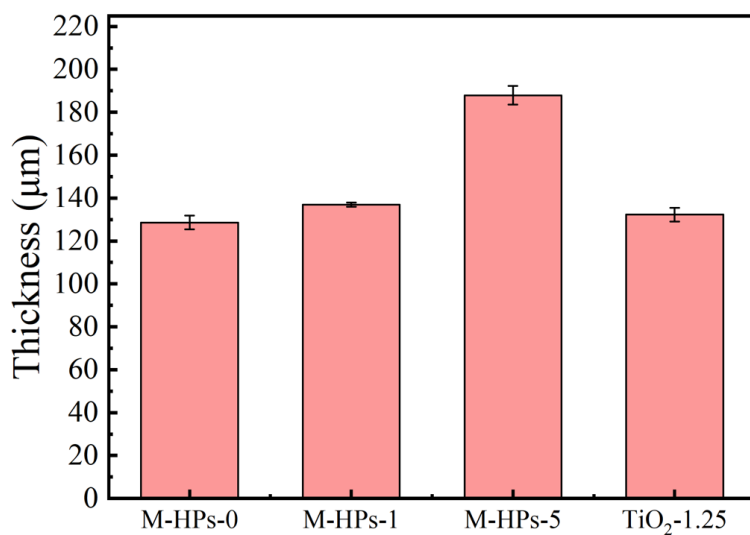
119



120

121 **Fig. S5.** The viscosity of electrospinning solutions.

122

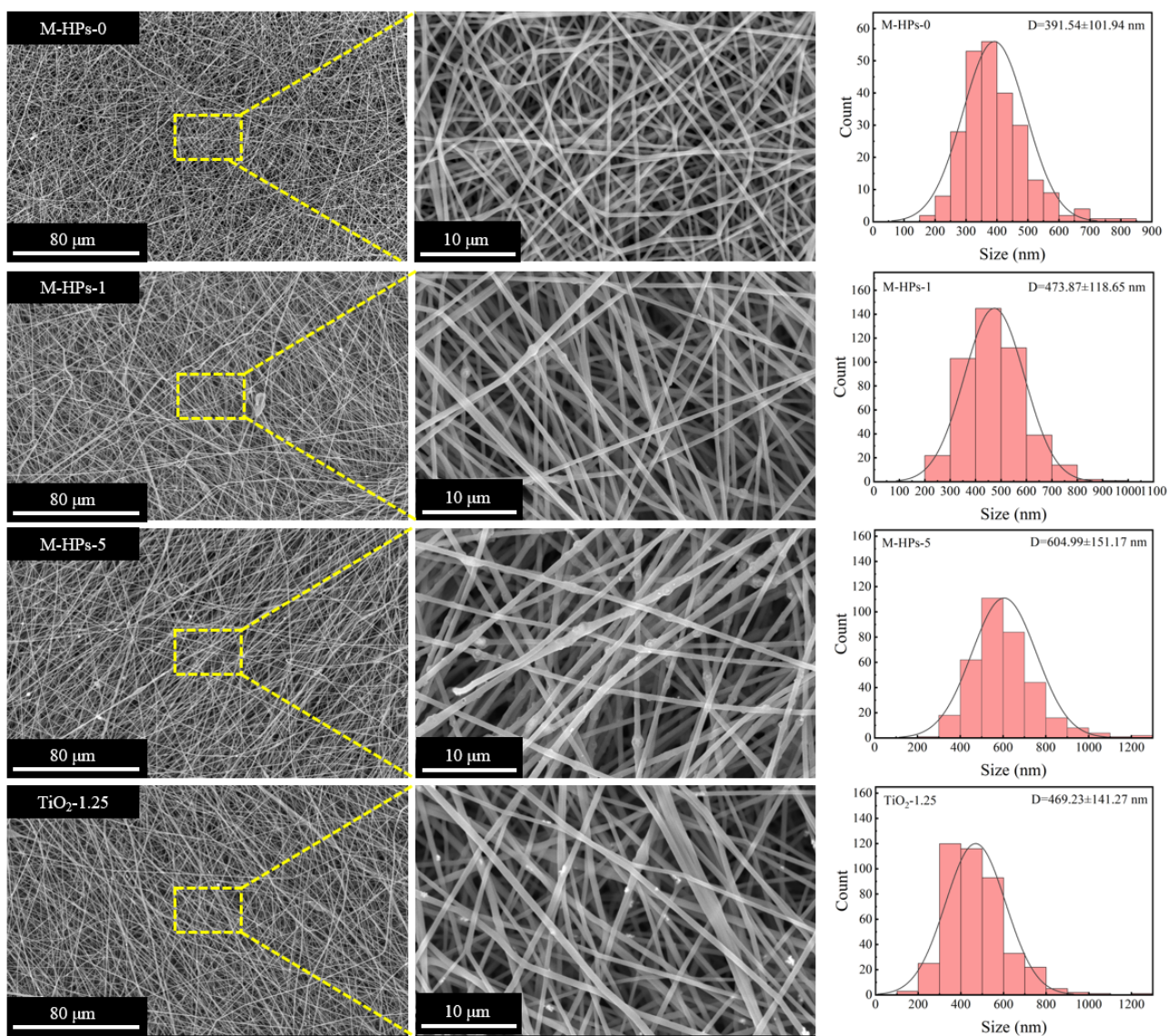


123

124 **Fig. S6.** The thickness of PAN/M-HPs NFMs and PAN/TiO<sub>2</sub> nanoparticle NFM.

125



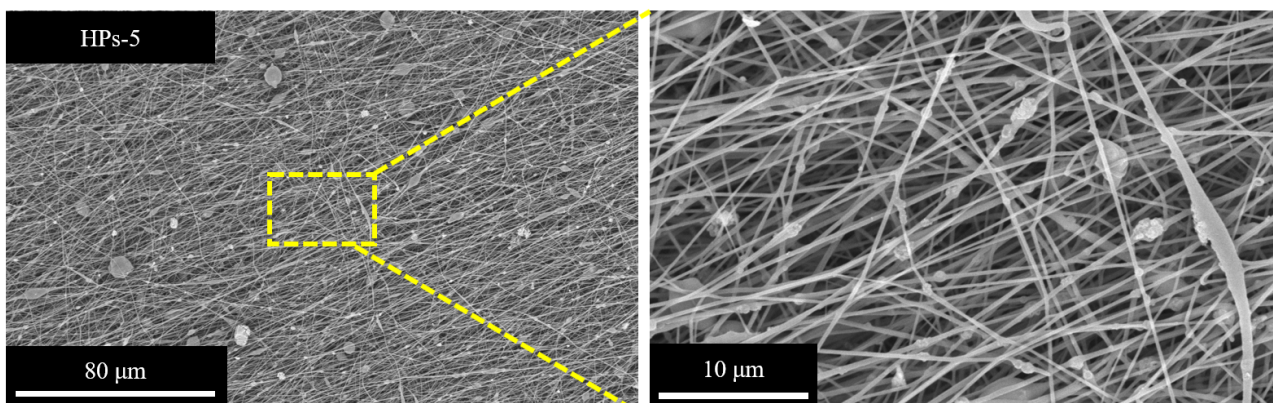


126

127 **Fig. S7.** The SEM images (500× and 3000× magnification) and fiber diameter distributions of PAN/M-

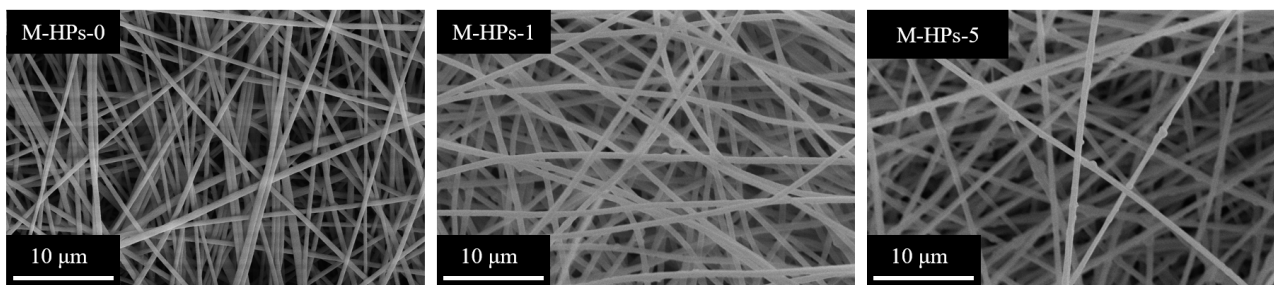
128 HPs NFMs and PAN/TiO<sub>2</sub> nanoparticle NFM.

129



130

131 **Fig. S8.** The SEM images of HPs-5 NFM (500× and 3000× magnification).



132

133 **Fig. S9.** The SEM images of PAN/M-HPs NFMs after three washing-drying cycles (3000× magnification).

134

## 135 **References**

136 1. K. Liu, L. Deng, T. Zhang, K. Shen and X. Wang, *Ind. Eng. Chem. Res.*, 2020, **59**, 4447-4458.